

# Very long distance connection of gigawatt-size offshore wind farms: extra high-voltage AC versus high-voltage DC cost comparison

Stefano Lauria<sup>1</sup>, Maddalena Schembari<sup>1</sup>, Francesco Palone<sup>2</sup>, Marco Maccioni<sup>1</sup> ✉

<sup>1</sup>DIAEE Department, 'Sapienza' University of Rome, Via Eudossiana n° 18, 00184 Rome, Italy

<sup>2</sup>TERNA Rete Italia S.p.A., Via Marcigliana n°911, 00138 Rome, Italy

✉ E-mail: marco.maccioni@uniroma1.it

ISSN 1752-1416

Received on 27th July 2015

Revised on 17th November 2015

Accepted on 19th December 2015

doi: 10.1049/iet-rpg.2015.0348

www.ietdl.org

**Abstract:** This study presents a cost comparison between commercially available high-voltage DC (HVDC) and extra high-voltage AC shore connection ( $\pm 320$  kV voltage source converter and 420 kV–50 Hz single-core and three-core cables), for a 1 GW offshore wind farm cluster, considering transmission distances up to 400 km. The HVDC system is a point-to-point connection whereas multiple AC intermediate compensating stations are envisaged for AC when needed. Capital costs are evaluated from recently awarded contracts, operating costs include energy losses and missed revenues due to transmission system unavailability, both estimated using North Sea wind production curves. Optimal AC intermediate compensation, if any, and reactive profiles are also taken into account. Results show that HVDC has lower transmission losses at distances in excess of 130 km; however, due to the combined effect of lower AC capital cost and unavailability, using three-core aluminium cables can be more convenient up to 360 km distance.

## 1 Introduction

In the year 2014, 1713 MW of offshore wind plants have been installed all over the world, pushing the global capacity up to 8759 MW. More than 91% of all offshore wind installations (8045 MW) are in European waters (mainly in the North Sea), where, in 2014, 1483 MW of new offshore wind capacity were connected. There are now 74 offshore wind farms (OWFs) in 11 countries across Europe, capable of producing 29.6 TWh in a normal wind year; enough to cover 1% of the European Union's total yearly electricity consumption. Such fast development has recently slowed down, also due to financial and technical issues related to shore connection and especially offshore converter stations.

The 12 projects currently under construction in Europe will bring the cumulative offshore wind capacity in Europe to 10.9 GW in the course of 2015–2016. Beyond 2016, European Wind Energy Association has identified 26.4 GW of authorised OWFs in Europe, with future plans for more than 98 GW [1]. Given the involved capacities, the evolution of the point-to-point offshore connections into a meshed grid ('supergrid') with the ultimate aim of interconnecting the North Sea seaboard countries is ultimately envisaged in the long term.

The emergence of larger individual wind turbine ratings (8 MW offshore units under test) drives a continuous increase of OWF capacity: at present, the world's largest OWF is 630 MW London Array. Besides simpler and faster permitting procedures compared to land-based wind farms, OWFs farther from shore enjoy better wind conditions, so that in the next few years the aggregation of several OWFs of even larger size into clusters with a capacity of several gigawatts (GWs), at distances from shore in the order of 100 km, is expected.

With the increase of rating and distances, the impact on total costs of the transmission solution adopted to connect OWFs to the mainland grid becomes very significant, so special attention must be paid to the choice of the technology to be adopted, either high-voltage DC (HVDC) using voltage source converters (VSC-HVDC) or high-voltage AC (HVAC).

Until recently, HVAC (145–245 kV) transmission was chosen for the majority of OWFs, generally not farther than few tens of kilometre from shore. However, in the last few years, VSC-HVDC

was preferred for the connection of new long-distance OWFs, following the opinion that the break-even distance for such power links was about 80 km [2, 3]. Such conviction was due to the constraints on HVAC cable line (CL) length brought by the hydraulic circuit of then-standard self contained fluid-filled cables, which were the state-of-the-art of extra HVAC (EHVAC) cables before the introduction of EHV cross-linked polyethylene (XLPE) insulation in the 1990's, as well as by the intrinsic length limit of any AC CL due to its own reactive power surplus [4].

The above cited limits do not affect HVDC lines since most HVDC cables do not contain liquid insulation. Moreover, VSC-HVDC has some significant potential advantages, such as active and reactive power controls, frequency decoupling between OWF and onshore grid and black-start capability. However, VSC-HVDC is not a fully mature technology, service experience being limited to a few systems, and offshore converter stations have notably experienced problems (e.g. Borwin 1 VSC), 'inducing anxiety (and caution among investors) about using HVDC in a relatively untried environment' [5].

In the same time span, HVAC cable technology underwent significant improvements with the adoption of XLPE insulation, which suppresses length constraints related to oil circuits. Moreover, the derating effect of reactive power is lessened by the smaller dielectric constant and greater thickness of XLPE compared with paper-oil insulation, yielding a smaller capacitance; this is compounded by the higher operating temperature of XLPE, which can result in a higher ampacity. In the field of submarine transmission, applications to this date are mostly at voltages not exceeding 245 kV; 420 kV–50 Hz XLPE submarine cables are, however, in service. Thanks to the aforementioned technical advances, the maximum feasible length of AC CLs has substantially increased, with one submarine CL longer than 100 km presently in commercial service, i.e. the 245 kV–50 Hz Malta–Sicily link, 120 km long [6].

Following the commissioning of the Malta–Sicily interconnector, HVAC has been also chosen for the connection of some ongoing, long distance OWF projects:

- East Anglia 1 (714 MW), involving a 420 kV–100 km long submarine export link [7].

- West of Adlergrund (250 MW) involving a 245 kV–90 km long submarine export cable [8].

To fully exploit such long CLs, i.e. to achieve a high active power loading, the line must be operated with a symmetrical reactive power profile (by means of appropriate terminal voltage control), thus maximising its active power transfer capability and minimising joule losses. Calculations show that in such an operating condition a single circuit of 420 kV three-core cable could transfer up to 500 MW at 90 km distance [9].

Further extensions of the AC transmission distance are granted by the installation of reactive compensation at intermediate locations along the cable route: appropriate compensation actually allows multiplying the maximum line length [10]. Intermediate compensations (ICs) of a HV/EHV submarine CL require additional offshore platforms, which might be feasible in the relatively shallow seabed of the North Sea.

From the economic point of view, both manufacturing and laying costs of AC submarine cables have been brought down by the introduction of three-core XLPE-insulated cables which can use galvanised steel armour, inexpensive if compared with the copper armour which is required by single-core AC cables in order to keep losses at an acceptable level.

Present-day AC submarine cable technology could make HVAC competitive with VSC-HVDC for the interconnection of GW-sized OWFs at distances from shore exceeding 100 km (or more, considering the use of intermediate compensation), suggesting the need for an up-to-date cost comparison between the two technologies, including capital costs and capitalised energy losses (line losses and outages).

The paper deals with the assessment of total costs associated to VSC-HVDC and EHVAC options for the connection of a GW-sized OWF cluster at a distance from shore up to several hundreds of kilometres.

Different solutions for the shore connection, based on VSC-HVDC or EHVAC, are outlined, assuming the distance from shore as a parameter. For the AC case, operation with an optimised voltage/reactive power profile is simulated; use of intermediate reactive compensation is also considered as a design option (becoming a technical necessity with the increase of transmission distance). The HVDC case is a straightforward point-to-point connection. Besides the estimated capital investments, operating costs are calculated by capitalising energy losses and energy not supplied (ENS) due to outages of the transmission system.

The possible options adopted for the test system are introduced in Section 2, along with some general recalls on HVAC cables; Section 3 deals with the assessment of capital and operating costs associated to each solution. The economic comparison is reported in Section 4.

## 2 Design options and sizing

Long HV/EHV AC cables have a distinctive power-length relationship due to the derating effect of their inherent reactive power surplus, causing a decrease of transmissible power as line length increases. The power transmission capacity is maximised when the reactive power profile along the CL is symmetrical: for a homogeneous cable stretch without in-line shunt compensation the relationship between maximum active power transmission and line length is given, in the lossless approximation, by Gatta *et al.* [11]

$$P_{\max}(L) = S_z \cdot \sqrt{1 - \left[ \frac{P_c^2 - S_z^2}{2P_c S_z} \tan(K''L) \right]^2} \quad (1)$$

where  $P_{\max}$  is the maximum active power transfer capacity,  $P_c$  and  $S_z$  are, respectively, the surge impedance loading (SIL) and the apparent power at thermal limit of the line (MW) calculated at the same voltage  $U$ , common to both CL terminals,  $K'$  is the imaginary part of the propagation constant ( $\text{km}^{-1}$ ) and  $L$  is the CL length (km).

It should be pointed out that the usual line-end compensation does not affect the  $P$ – $L$  relationship (1). It can be shown that installation at mid-line of aptly sized inductive shunt compensation splits the CL in two, with regard to the reactive power surplus. Neglecting losses, the required mid-line compensation evaluated at the same voltage  $U$  used in (1) is [12]

$$Q_{\text{IC}} = \frac{P_c^2 - S_z^2}{P_c} \tan\left(K'' \frac{L}{2}\right) \quad (2)$$

with equal terminal voltages  $U$ .

Each of the resulting half-length CL segments behaves as a standalone line, with a higher  $P_{\max}(L/2)$  compared with the original line of length  $L$ . A larger power can thus be transferred over the same distance and, conversely, the maximum transmission distance for a given target power can be increased up to  $2L$ . Extending the concept to the case of  $n$  intermediate compensating stations, the maximum line length for a given power  $P$  can attain in theory  $(n+1)L$  [10].

For the purposes of the present paper, the maximum distance over which a given AC CL can transfer the 1 GW target active power without resorting to intermediate compensation is defined as ‘base’ length,  $L_{\text{Base}}$ , keeping in mind the task of evacuating to shore the output of a 1 GW OWF and the results of previous studies [9, 13, 14], two EHVAC (420 kV–50 Hz) alternatives have been evaluated.

AC scenario #1 is based on a double-circuit CL made of three-core, 1400 mm<sup>2</sup> aluminium cables. As shown in [9], one circuit of such cable can transfer 500 MW at distances up to 90 km without intermediate shunt compensation ( $L_{\text{Base1}} = 90$  km). Transmission distances up to 180 km can be attained with one intermediate compensating station; two such stations are required in the (181–270)km range and three in the (271–360)km interval.

AC scenario #2 is based on a single-circuit CL with 2000 mm<sup>2</sup> copper cables, having  $L_{\text{Base2}} = 100$  km [10, 11]. One intermediate station is envisaged for distances in the (101–200) km range and two for (201–300) km.

The case with three intermediate compensating stations, theoretically enabling target power transmission at distances up to 400 km, was not simulated. This is due to onset of a further constraint on CL operation concerning voltage regulation along the line, besides the usual thermal considerations. If the CL is operated with a symmetrical reactive power profile along each homogeneous line stretch, the voltage drop practically coincides with its resistive component yielded by the short-line approximation [11]

$$\Delta U_{\text{SR}} = \frac{R_C \cdot P_R}{U_R} \quad (3)$$

where  $R_C$  is the CL resistance,  $P_R$  and  $U_R$  are, respectively, the active power and the voltage at receiving end. It can be easily verified that  $\Delta U_{\text{SR}}$  from (2) is just a few kV for the cases with no intermediate compensation, i.e. 90–100 km CLs; longer configurations quickly yield  $\Delta U_{\text{SR}}$  values in excess of 20 kV at full load, making prolonged operation impossible when the receiving-end voltage is over 400 kV. The three-compensations, 400 km case in scenario AC#2 falls under this constraint.

Several cases have been considered for each scenario: four (base cases) reproduce systems having a length, respectively, equal to  $L_{\text{Base}}$ ,  $2 \cdot L_{\text{Base}}$ ,  $3 \cdot L_{\text{Base}}$  and  $4 \cdot L_{\text{Base}}$ , and a number of intermediate stations corresponding to the minimum required for each of these lengths (0, 1, 2 and 3, respectively). In order to thoroughly evaluate the impact of intermediate compensation on total costs, three additional cases have been considered, respectively envisaging  $L_{\text{Base}}$ ,  $2 \cdot L_{\text{Base}}$  and  $3 \cdot L_{\text{Base}}$  with 1, 2 and 3 intermediate stations (i.e. one more than the minimum needed for each length).

The simulated system originates from a 400/155 kV autotransformer (ATR) on the offshore collection platform, connecting OWF HV collection system to the EHV transmission line. For AC#1 scenario, two 500 MVA ATRs are installed, allowing for independent operation of the two submarine links; for

**Table 1** ATRs' data

$U_1/U_2$ , kV/kV	$S_n$ , MVA	$V_{scr}$ %	$P_{scr}$ kW	$P_0$ , kW
400/155	500	12.5	650	112
400/155	1000	12.5	1300	224

AC#2 scenario, a single 1000 MVA ATR has been considered. ATRs nameplate data are reported in Table 1, where  $U_1/U_2$  is the turns ratio,  $S_n$  is the apparent power,  $V_{sc}$  is the short-circuit voltage and  $P_{sc}$  and  $P_0$  are the copper and iron losses, respectively.

Simulated AC scenarios are summarised in Table 2, which also reports overall values of intermediate and terminal compensations (respectively,  $Q_{IC\_TOT}$  and  $Q_{TC\_TOT}$ ) for each HVAC case.

**Table 2** Simulated AC scenarios

	AC#1				AC#2			
	Length, km	# of IC stations	$Q_{IC\_TOT}^a$ , Mvar	$Q_{TC\_TOT}^a$ , Mvar	Length, km	# of IC stations	$Q_{IC\_TOT}^a$ , Mvar	$Q_{TC\_TOT}^a$ , Mvar
base cases	2 × 90	0	0	4 × 475	100	0	0	4 × 280
	2 × 180	1	4 × 475		200	1	4 × 280	
	2 × 270	2	8 × 475		300	2	8 × 280	
	2 × 360	3	12 × 475		–	–	–	–
additional cases	2 × 90	1	4 × 230	4 × 230	100	1	2 × 270	2 × 270
	2 × 180	2	8 × 310	4 × 310	200	2	4 × 365	2 × 365
	2 × 270	3	12 × 350	4 × 350	300	3	6 × 415	2 × 415

<sup>a</sup>Three-phase rating, at 420 kV

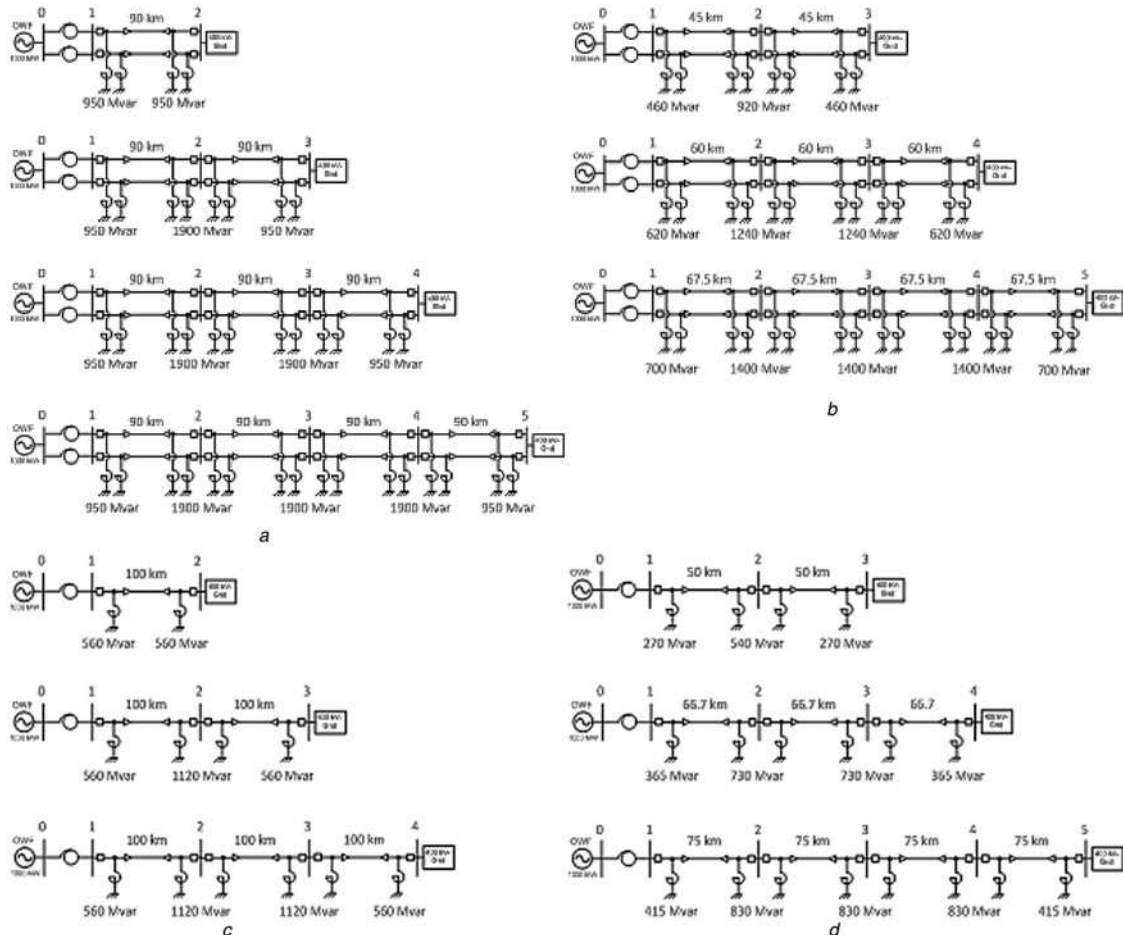


**Fig. 1** Single-line diagrams of AC simulated system configurations

- a AC#1 base cases
- b AC#1 additional cases
- c AC#2 base cases
- d AC#2 additional cases

Intermediate shunt compensation is sized according to [12], in all cases. Fig. 1 reports single-line diagrams of the simulated configurations.

The choice of the HVDC-VSC solution is more straightforward: based on commercially available technology, a  $\pm 320$  kV, 1000 MW system was considered, in conjunction with  $1950 \text{ mm}^2$  Cu cables (in order to have a  $0.8 \text{ A/mm}^2$  current density at full load).

For each AC scenario, an HVDC alternative has been considered, i.e. a classic point-to-point connection between the OWF collection platform and the onshore network by means of a single DC link. Transmission distances in the 0–400 km range are well within the feasible range for existing HVDC submarine transmission using line-commutated converters (LCCs) submarine transmission, similar line lengths are also envisaged for future VSC-HVDC



**Table 3** Main electrical characteristics of simulated cables

Design option	Cable	Insulation	$r', \Omega/\text{km}$	$\chi^a, \Omega/\text{km}$	$c', \text{nF}/\text{km}$	$I_z, \text{A}$
AC #1	1400 mm <sup>2</sup> Al	XLPE	0.0425 <sup>b</sup>	0.125	190	945
AC #2	three-core 2000 mm <sup>2</sup> Cu single core	XLPE	0.0255 <sup>b</sup>	0.072	208	1620
DC	1950 mm <sup>2</sup> Cu	XLPE	0.011 <sup>c</sup>	–	–	1560

<sup>a</sup>At 50 Hz<sup>b</sup>AC resistance at 90°C<sup>c</sup>DC resistance at 70°C

submarine projects. Table 3 reports main electrical parameters of selected cables, taken from manufacturer data sheets or estimated; ampacities  $I_z$  are indicative.

### 3 Cost assessment

#### 3.1 Capital costs

Investment costs associated to each scenario have been assessed based on economic data on ongoing or completed projects, collected from technical literature, transmission system operators' (TSOs) documentation and tender results. AC capital costs include, besides cables, terminal station equipment (line bays, transformers, and shunt reactors) and intermediate compensation (platforms and reactors) when present. EHVAC cable costs have been taken from recently awarded contracts [15] or conservatively estimated from AC submarine cables having similar rating [16, 17]. Values are turnkey costs, including transportation, laying, protection and testing.

Station equipment weights and costs refer to Terna standards and, respectively, average costs [17]. A gas insulated substation (GIS) double-busbar, single circuit breaker (CB) switching scheme was assumed in all stations; shunt reactors have been considered solidly connected to the CL terminals. Offshore platform housing intermediate shunt compensation costs have been estimated as a function of equipment weight according to [18], also used to assess the cost of reactors at the terminal stations.

DC capital costs are due to cables and converter stations. DC cable costs [€/MW km] were estimated by averaging available cost figures from the most recent bidding data for ±320 kV XLPE-insulated submarine DC cables (see Table 4). All these values are turnkey costs. The 1.95 M€/GW km cost has been rounded to 2 M€/GW km, as reported in Table 5: this value is very similar to the one estimated in [23], in which prices range from 1.395 M€/km (i.e. about 1.95 M€/km) to 1.52 M€/km (i.e. about 2.13 M€/km) for a 1 GW DC cable system, depending on the trenching arrangement.

Table 5 resumes cable costs for the different design options.

Converter station costs have been estimated considering a 220 M €/GW cost for the offshore converter station and 92 M€/GW cost

**Table 4** Data on VSC-HVDC projects employed for the assessment of DC cable cost

	Length, km	Rated power, MW	Cost, M€	Cost, M €/GW · km	Average cost, M€/GW · km
Silwin 1 [19]	204	864	250	1.418	1.95
Dolwin 3 [20]	161	900	350	2.415	
Helwin 2 [21]	130	690	200	2.230	
Borwin 3 [22]	160	900	250	1.736	

**Table 5** Cable costs for each design option

Design option	Cable	Cost, M€/km
AC #1	1400 mm <sup>2</sup> Al three-core, double circuit	2.0
AC #2	2000 mm <sup>2</sup> Cu single-core, single circuit	3.0
DC	1950 mm <sup>2</sup> Cu	2.0

for the onshore one [24]. All the above capital costs are plotted in Fig. 2 as a function of the distance from shore.

Curves in Fig. 2 follow the expected patterns: DC capital cost has a large initial offset due to converter stations but a smaller slope than AC curves. Discontinuities of AC cost functions are due to additional compensating stations at integer multiples of  $L_{\text{Base}}$ . Cost steps due to compensation are smaller for the single-circuit AC solution #2; however due to the higher cost of single-core AC copper cables, DC achieves breakeven at about 180 km. The most remarkable feature of Fig. 2 is that thanks to the relatively inexpensive aluminium cables, AC solution #1 has a lower capital cost than DC up to 360 km length.

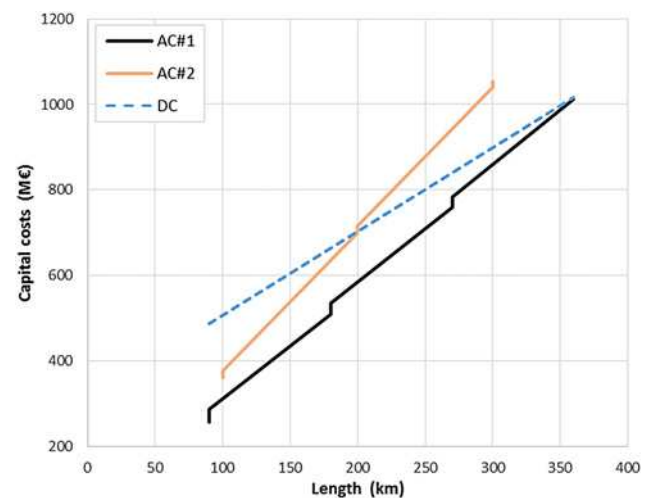
#### 3.2 Operating costs

Operating costs include maintenance costs and capitalised missed revenues due to power losses and outages. Maintenance costs have been actualised and included in above-mentioned capital costs: this can be a reasonable scenario involving a complete turnkey engineering, procurement, construction and installation and maintenance contract for the overall project. Total ENS is the sum of transmission losses and energy not delivered due to link outages.

**3.2.1 Availability:** Wind farms have a limited economic lifetime due to both technical and economic/financial issues (especially when considering the 'optional acceleration model' for remuneration, see Section 3.2.3). ENS due to link outages can have a detrimental impact on project economics, as recently demonstrated by recent faults in HVDC-connected wind farm arrays [25, 26], so that reliability must be considered as one of the main criteria for design and cost evaluation of the link.

For both AC and DC solutions, redundant design criteria, as well as adequate safety margins on equipment rating and proper maintenance, can significantly reduce the risk of outages, at the expense of higher capital and operational costs.

A first estimate of the expected energy availability of the link can be obtained by considering the service experience statistics of substation components (HVDC converter, transformers and GIS)

**Fig. 2** Capital costs of the different scenarios versus total interconnector length

**Table 6** Failure rate of submarine cable systems (from [25])

	AC-SCOF CABLES			AC-XLPE CABLES			DC-MI CABLES		
	60–219 kV	220–500 kV	all voltages	60–219 kV	220–500 kV	all voltages	60–219 kV	220–500 kV	All voltages
failure rate (fail/year·100 cct km)									
internal origin failures	0.0000	0.0000	0.0000	0.0000	N.A. <sup>a</sup>	0.0000	0.0000	0.0000	0.0000
external origin failures	0.1277	0.0738	0.1061	0.0705	N.A. <sup>a</sup>	0.0705	0.1336	0.0998	0.1114
all failures	0.1277	0.0738	<b>0.1061</b>	0.0705	N.A. <sup>a</sup>	<b>0.0705</b>	0.1336	<b>0.0998</b>	0.1114

<sup>a</sup>Not available

and submarine cable reliability data. Under this regard CIGRE statistics [27–29] represent the most significant data collection.

Due to the lack of long term reliability data of VSC-HVDC converters, especially in offshore applications, onshore HVDC LCC converter stations average energy availability values [30] have been considered. Although LCC converter stations include larger filters than those required by VSC stations (if any), the use of LCC reliability data should lead to an overestimation of offshore converters energy availability, mainly due to the larger expected mean time to repair (MTTR) of offshore plants compared with land-based ones. Depending on the affected component, two main fault categories have been considered, ‘cable’ and ‘station’ faults, as described as follows.

**Cable faults:** Cable faults can have internal (dielectric faults) as well as external (anchoring, fishing) causes. Accurate cable testing and prequalification significantly reduce the former, whereas proper mechanical protection along the whole cable route (in relatively shallow waters) is expected to minimise the latter.

Cable failure rates from [27] are summarised in Table 6. For XLPE AC submarine cables a value of 0.0705 fail/year·100 cct km is reported; however, this value refers to voltages below 220 kV, due to the lack of service experience of EHVAC XLPE cables, and mainly to three-core cables. Hence, in order to avoid to underestimate the failure rate of single-core copper cables, the value for self-contained oil-filled (SCOF) cables (0.1061 fail/year·100 cct km), most of which are single-core, is taken into account. According to [27], SCOF cables experience fewer internal failures than XLPE-insulated ones; however, statistics show that submarine cable faults have nearly always an external cause. For the same reason, the above reported figure about XLPE cables is suitable for the three-core aluminium cable, in spite of referring to lower-voltage levels.

As regards DC cables, the 0.0998 fail/year·100 cct km value of mass impregnated (MI) DC cables has been considered due to lack of service experience regarding submarine cables with extruded insulation. This assumption is likely to underestimate the failure rate of XLPE HVDC cables, which use a relatively new technology compared with MI ones.

For all cases, a 60 days MTTR has been considered [27]; use of spare cables have not been considered in any connection solution. For both the HVDC-VSC (symmetrical monopole) and AC#2

(single-circuit CL), a cable fault causes a complete link outage, whereas for AC#1 (double-circuit CL), a fault causes a 50% reduction in power transmission capability, at most.

**Station faults:** For AC station equipment, the following fault rates have been considered:

- GIS bay equipment failure (0.36 fault/100 CB-bay-years) [28] and
- ATR or shunt reactor failure (1 fault/100 transformers·year) [29].

The MTTR has been assumed as 60 days for GIS, transformers and shunt reactors. This value is an average between major faults (site inspection and/or site repair) and equipment replacement.

As regard to shunt reactor failure, a single fault implies the outage of the attendant cable circuit, thus causing a 50% reduction of transmission capacity for the three-core solution and a 100% reduction for the single-core case. Only failure rates related to offshore shunt reactors are considered, assuming that a spare unit is always available in the onshore substation.

For the DC system, the aggregate energy unavailability of both converter stations has been taken at 3.63% [30]; this includes all station components, such as GIS, transformers, filters, and so on.

Table 7 resumes values of unavailability calculated for each scenario.

**3.2.2 Transmission losses:** AC transmission losses are calculated based on power flow calculations, as the difference between input and output powers of the whole system. They include joule and dielectric losses of each cable stretch, as well as shunt reactor and transformer losses (transformer nameplate data are reported in Table 1; shunt reactor losses are simulated with a quality factor  $q=600$ ). AC cable resistance is conservatively assumed at maximum service temperature (90°C) for all operating regimes.

Assuming 400 kV as receiving-end voltage in all cases, calculations were carried out by adjusting the sending-end voltage for every operating point, in order to ensure the aforementioned symmetrical current-reactive power profile along each individual cable stretch [11, 13, 14], thus maximising AC cable loadability and transmission efficiency. In order to reduce losses at low load, switching-off of one circuit at loads below 50% of rating is assumed in AC#1 scenario.

**Table 7** Unavailability values of simulated scenarios

	Cases		Unavailability, %					
	Length, km	# of IC stations (for AC)	AC			DC		
			Cables	Substations	Total	Cables	Substations	Total
AC #1 (for each circuit)	90	0	1.043	0.447	1.490	1.48	3.63	5.11
	90	1	1.043	0.894	1.937			
	180	1	2.096	0.894	2.980	2.95	3.63	6.58
	180	2	2.096	1.341	3.427			
	270	2	3.139	1.341	4.470	4.43	3.63	8.06
	270	3	3.139	1.788	4.918			
AC #2	360	3	4.172	1.788	5.961	5.91	3.63	9.54
	100	0	1.744	0.447	2.191	1.64	3.63	5.27
	100	1	1.744	0.894	2.638			
	200	1	3.488	0.894	4.382	3.28	3.63	6.91
	200	2	3.488	1.341	4.830			
	300	2	5.232	1.341	6.574	4.92	3.63	8.55
	300	3	5.232	1.788	7.021			

HVDC transmission losses are the sum of converter station losses and DC cable losses; lacking further information, especially regarding the recently introduced modular multi-level converters, station losses are taken as linearly variable with load, i.e. equal to 1% of transmitted power in every operating regime.

DC cable losses have been calculated using the equation [31]

$$\text{Losses (\%)} = \frac{J \cdot \rho \cdot l}{10 \cdot U_o} \quad (4)$$

where  $J$  is the current density ( $A/mm^2$ ),  $\rho$  the resistivity at operating temperature ( $\Omega \text{ mm}^2/km$ ),  $U_o$  the operating line-to-ground voltage (kV) and  $l$  the line length (km). The  $\rho$  value has been conservatively taken at  $21.6 \Omega \text{ mm}^2/km$ , i.e. at  $70^\circ C$  temperature for all operating regimes; DC receiving-end voltage has always been set at 1 pu, i.e.  $\pm 320 \text{ kV}$ , as implied by (4). Fig. 3 shows transmission losses, as a percentage of transmitted power, plotted against OWF output for the base cases of each scenario.

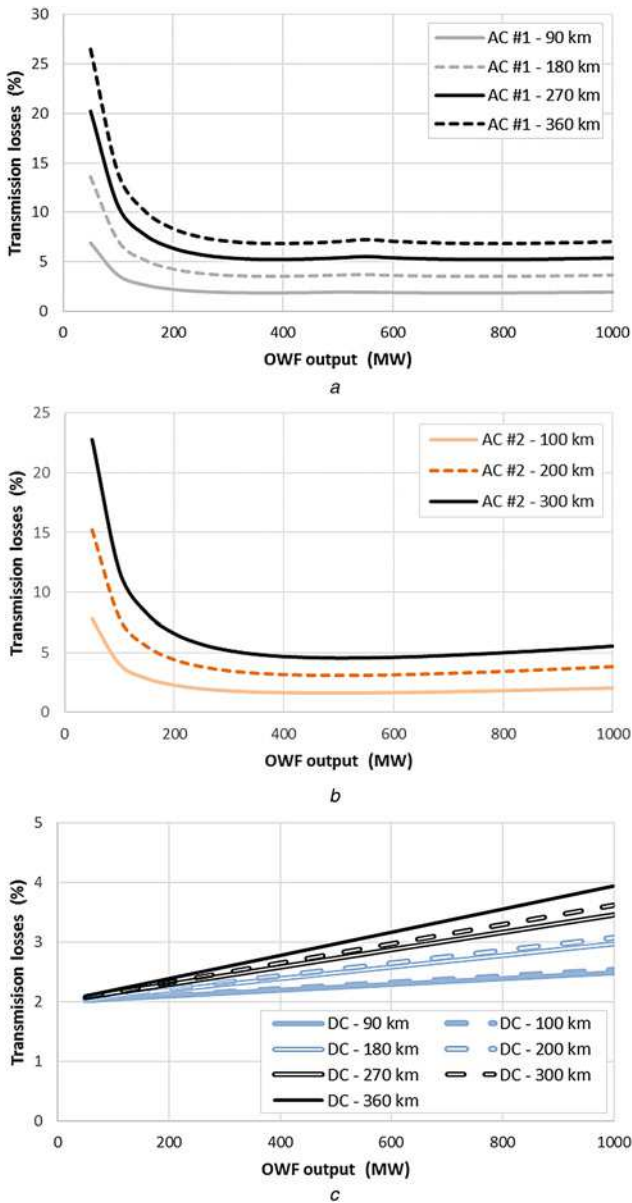


Fig. 3 Transmission losses against OWF output for base cases

- a AC #1
- b AC #2
- c DC

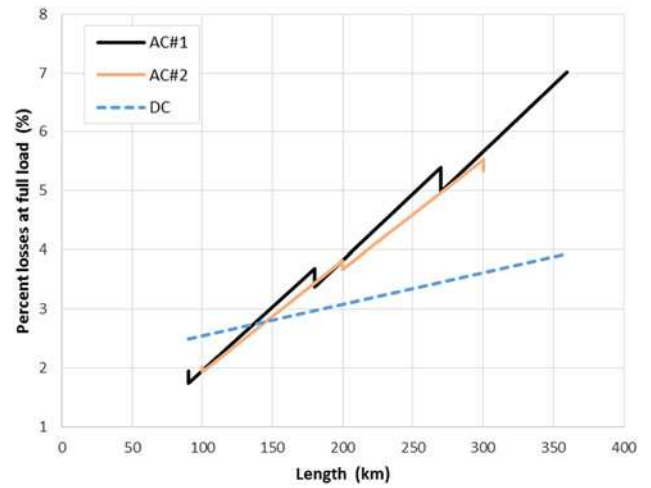


Fig. 4 Transmission losses at full load versus total interconnector length, for each scenario

Discontinuities in AC#1 curves at 50% of OWF output are due to the switching-off of one circuit below this value.

Fig. 4 shows total losses at full load as a function of transmission distance; curves highlight the beneficial effect of intermediate compensation on transmission losses, which is more pronounced in the AC#1 scenario due to the higher losses of the aluminium cable (loss reduction is 10.7, 8.5 and 7.6%, respectively, for 90, 180 and 270 km case). With AC#2 copper cables the decrease is between 4.6% and 3.6%. HVAC full-load losses are lower than in the DC case until about 135 km for the AC#1 scenario, and about 150 km for AC#2.

**3.2.3 Economic value of total ENS:** To calculate the total amount of the energy yearly supplied (EYS), the OWF yearly energy production is assessed as in [9], combining wind probability distribution data on an hourly basis from the wind atlas of the Dutch part of the North Sea and equivalent wind turbine power curves [32]. The OWF power output  $P$  is assumed variable from 10 to 1000 MW, with a 10 MW step  $\Delta P$

$$P_j = j \cdot \Delta P, \quad j \in (1, 100) \quad (5)$$

Transmission losses over a year are calculated for all design alternatives as a function of OWF output. With regard to the generation scenario with a nil OWF power output, some clarifications are needed. The calculation of the net balance of the system during no-generation periods depends on the adopted operating mode. Keeping the system connected to the grid, a certain amount of energy will be drawn from the grid for auxiliaries' consumption and no-load losses. In turn, the cost of such eventual energy will depend on several factors such as the ownership of the transmission system as well as specific market rules and/or commercial agreements with local TSO. Hence, at this stage of the study, during no-generation periods switching-off of the whole system is assumed as a hypothesis, resulting in a nil net energy balance.

The EYS value of each case is calculated based on the following expression

$$\text{EYS(MWh)} = \left( \sum_{j=1}^{100} (P_j - p_j) \cdot h_j \right) \cdot (1 - u) \quad (6)$$

where  $p_j$  is the power loss corresponding to a  $P_j$  active power transfer,  $h_j$  is the yearly number of hours at  $P_j$  and  $u$  is the unavailability value of the considered case, taken from Table 7.

The total amount of energy yearly not supplied (EYNS) can be assessed as the difference between the OWF yearly energy output

$P_j \cdot h_j$  and the EYS

$$\text{EYNS(MWh)} = P_j \cdot h - \text{EYS} \quad (7)$$

The above method is applied to AC#2 and DC scenarios. For the AC#1 case, the total EYS is calculated as the sum of two components, i.e. the EYS transmitted in sound conditions and the EYS transmitted with one faulted circuit out of two

$$\text{EYS(MWh)} = \text{EYS}_{2\text{circuits}} + \text{EYS}_{1\text{circuit}} \quad (8)$$

The first term is calculated considering the probability  $(1 - 2u + u^2)$  that the two circuits are both sound, as

$$\text{EYS}_{2\text{circuits}}(\text{MWh}) = \left( \sum_{j=1}^{100} (P_j - p_j) \cdot h_j \right) \cdot (1 - 2 \cdot u + u^2) \quad (9)$$

Switching-off of one of the two circuits with generation output below 50% of the OWF power rating (500 MW) is considered in order to enhance transmission efficiency [9]. The second component of total EYS can be assessed considering the probability that only one of the circuits undergoes an outage, i.e.  $2 \cdot (u - u^2)$ . For all generation scenarios with  $P_j$  above the power transfer capacity of the single circuit (i.e. 500 MW), the amount of generated power to be curtailed is added up to the transmission losses.

$\text{EYS}_{1\text{circuit}}(\text{MWh})$

$$= \begin{cases} \left( \sum_{j=1}^{50} (P_j - p_j) \cdot h_j \right) \cdot (2 \cdot u - 2 \cdot u^2) \\ \left( \sum_{j=51}^{100} (P_{50} - [(P_j - P_{50}) + P_{50}]) \cdot h_j \right) \cdot (2 \cdot u - 2 \cdot u^2) \end{cases} \quad (10)$$

The money value, i.e. the net present cost (NPC), of total ENS along the entire lifespan of the OWF for each considered case is assessed by means of the discounted cash flow method, according to the expression

$$\text{NPC(M€)} = \sum_{i=1}^N \frac{\text{EYNS} \cdot \text{PoE}}{(1 + d)^i} \quad (11)$$

The system's expected lifetime  $N$  is assumed equal to 40 years, whereas a relatively low discount rate  $d$  of 3.6%, typical of large energy utilities, is considered. As price of energy (PoE), the remuneration scheme included in the Renewable Energies Act, recently adopted by the German Parliament and the Federal Council is considered [33]: it foresees an initial remuneration of 194 €/MWh for a total of 8 years (so-called 'optional acceleration model') and a basic remuneration of 39 €/MWh for the following years.

## 4 Cost comparison

Fig. 5 reports the total NPC associated to each scenario, as a function of the interconnector length.

The AC#2 solution is less expensive than HVDC until about 240 km, while AC#1 is convenient in the entire length range and, possibly, until about 400 km. Discontinuities corresponding to the introduction of additional compensating stations are visible as in the case of capital costs (Fig. 2). However, for the AC#1 scenario they are less pronounced than in Fig. 2. This behaviour can be explained by looking at the part of NPC associated only to ENS (transmission losses and outages) in Fig. 5. For AC#1, the intermediate compensation acts towards a reduction of total energy

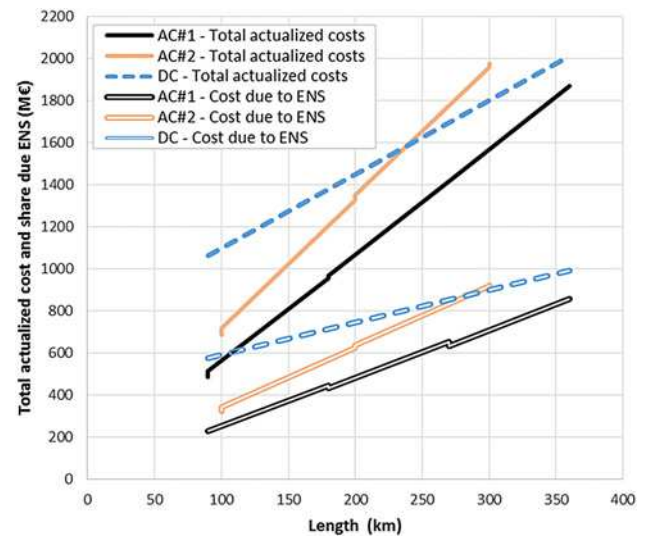


Fig. 5 Total net present cost for each scenario, versus total interconnector length

losses, whereas for AC#2 the effect is the opposite. In fact, despite the reduction in transmission losses granted by IC in both scenarios, although to different extents (see Fig. 4), the impact on outages is not the same. In both scenarios, an increased number of shunt reactors reduces the availability of the system: however, this worsening effect is less perceived in AC#1, due to the possibility to operate the link up to 50% of the rated power after the outage of one circuit, which substantially reduces total ENS. In other words, in the AC#1 scenario the reduction of transmission losses due to IC prevails on the increased probability of outages associated to it. For the single-circuit AC#2 scenario, the increased failure rate nullifies the benefit in terms of reduced transmission losses (which is also lower than for AC#1).

## 5 Conclusion

The paper discusses the assessment of capital and operating costs for to the transmission system of a hypothetical 1 GW OWF cluster. Three technical solutions, two employing EHVAC (420 kV–50 Hz) and one based on VSC-HVDC ( $\pm 320$  kV), are proposed. Taking the length of the interconnector as a parameter, investment cost and actualised ENS, due to transmission losses and unavailability of the system, have been calculated for each solution; an OWF lifespan of 40 years, a discount rate of 3.6% and a PoE of 194 €/MWh for the first 8 years and of 39 €/MWh for the rest of the lifespan are assumed. For the HVAC scenarios, operation with optimised voltage/reactive power profile is considered and limits on maximum feasible CL length are overcome by means of reactive power compensating stations along the route. The VSC-HVDC system is a conventional point-to-point line. Main results can be summarised as follows:

- Capital costs linearly increase with length in the HVDC case, whereas discontinuities corresponding to introduction of intermediate compensating stations are appreciable in AC cost functions. Despite the presence of intermediate compensation, breakeven with HVDC occurs at about 180 km for the single-core AC copper cable and 360 km for the double circuit of three-core AC aluminium cables.
- Outages data from statistics on service experience point out to higher failure rates for HVDC solution. In the HVAC scenarios, the introduction of intermediate compensation reduces system availability, due to the increased number of shunt reactors and GIS bays.
- AC transmission losses at full load are lower than those of DC for transmission distances not exceeding about 135 and 150 km,



respectively, for the single-core AC copper CL and the double circuit of three-core AC aluminium CL solutions. For a given length, intermediate compensation tends to reduce AC transmission losses, especially in the case with aluminium cables.

- For very long radial EHVAC interconnections, the sending-end voltage rise becomes a limiting factor at high active power loading.
- The advantage in terms of lower losses of HVDC-VSC option is significantly reduced by the higher probability of outages, which considerably affects the total amount of ENS.
- Evaluation of total NPC shows the convenience of HVAC solutions up until about 240 km for option AC#2 and 400 km for AC#1.

The study shows how technical progress along with proper design and operation can make EHVAC a viable alternative for the connection of GW-sized OWF at distances largely exceeding limit values usually associated to AC. Furthermore, the proposed economic analysis suggests the convenience of AC over DC in a wide range of transmission distances, when system availability is taken into account.

As a final remark, given the complex range of possible harmonic interactions to be found in both HVDC and HVAC long cable-based projects, detailed harmonic and transient studies involving the link (AC or DC), the receiving (continental) network and the OWF are always required, following technical–economical and steady-state analyses.

## 6 References

- 1 GWEC: 'Global wind report 2014', 2015. Available at <https://www.web.archive.org/web/20151011172649/http://www.gwec.net/publications/global-wind-report-2/global-wind-report-2014-annual-market-update/>
- 2 Bresesti, P., Kling, W.L., Hendriks, R.L., *et al.*: 'HVDC connection of offshore wind farms to the transmission system', *IEEE Trans. Energy Convers.*, 2007, **22**, (1), pp. 37–43
- 3 Van Eeckhout, B., Van Hertem, D., Reza, M., *et al.*: 'Economic comparison of VSC HVDC and HVAC as transmission system for a 300 MW offshore wind farm', *Eur. Trans. Electr. Power*, 2010, **20**, (5), pp. 661–671
- 4 Schiffreen, C.S., Marble, W.C.: 'Charging current limitations in operation of high-voltage cable lines', *AIEE Trans. III, Power Appar. Syst.*, 1956, **75**, pp. 803–817
- 5 Bell, K.R.W., Xu, L., Houghton, T.: 'Consideration in design of an offshore network', *CIGRE Sci. Eng.*, 2015, **1**, pp. 79–92
- 6 Lauria, S., Palone, F.: 'Optimal operation of long inhomogeneous ac cable lines: the Malta–Sicily interconnector', *IEEE Trans. Power Deliv.*, 2014, **26**, pp. 1036–1044
- 7 offshoreWIND.biz: 'East anglia one goes for HVAC transmission', 22 June 2015. Available at <https://www.web.archive.org/web/20151013123156/http://www.offshorewind.biz/2015/06/22/east-anglia-one-goes-for-hvac-transmission/>
- 8 Caruso, L., Caserta, L.: 'New award worth approximately € 230 M for offshore wind farm grid', Prysmian press release, Milano, Italy, 1 April 2015. Available at <https://www.web.archive.org/web/20151011172344/http://www.prysmiangroup.com/en/corporate/press-releases/New-award-worth-approximately-230-M-for-offshore-wind-farm-grid/>
- 9 Lauria, S., Maccioni, M., Palone, F., *et al.*: 'Cost evaluation of EHVAC offshore wind farm interconnections using intermediate shunt compensation: a parametric study'. Proc. IET ACDC 2015 Conf., Birmingham, United Kingdom, February 2015, pp. 1–6
- 10 Schiffreen, C.S., Dougherty, J.J.: 'Long cable lines – alternating current with reactor compensation or direct current', *AIEE Trans. III, Power Appar. Syst.*, 1962, **81**, pp. 169–178
- 11 Gatta, F.M., Geri, A., Lauria, S., *et al.*: 'Steady-state operating conditions of very long EHVAC cable lines', *Electr. Power Syst. Res.*, 2011, **81**, pp. 1525–1533
- 12 Gatta, F.M., Geri, A., Lauria, S., *et al.*: 'Steady-state operating conditions of very long EHVAC cable lines: two case studies', *Electr. Power Syst. Res.*, 2012, **83**, pp. 160–169
- 13 Lauria, S., Schembari, M., Palone, F.: 'EHV AC interconnection for a GW-size offshore wind-farm cluster: preliminary sizing'. Proc. IEEE Energycon 2014 Conf., Dubrovnik, Croatia, May 2014, pp. 1–6
- 14 Lauria, S., Schembari, M.: 'Voltage and reactive power control for maximum utilization of a GW-size EHVAC offshore wind farm interconnection'. Proc. Third IET RPG Conf., Naples, Italy, September 2014, pp. 1–6
- 15 Bawa, H.: 'ABB wins \$30 million order for world's highest voltage three-core AC subsea cable', ABB press release, Zurich, Switzerland, 13 February 2012. Available at <https://www.web.archive.org/web/20151007150000/http://www.abb.com/cawp/seitp202/6adf9ecaa8f5b962c12579a300395710.aspx>
- 16 Révillon, C.: 'Nexans wins a 171 million USD order to supply extra-high-voltage submarine link between Saudi Arabia and Bahrain', Nexans press release, Paris, France, 21 November 2005. Available at [https://www.web.archive.org/web/20151007133216/http://www.nexans.it/eservice/Italy-it\\_IT/navigatepub\\_155803\\_-3679/Nexans\\_wins\\_a\\_171\\_million\\_USD\\_order\\_to\\_supply\\_extr.html](https://www.web.archive.org/web/20151007133216/http://www.nexans.it/eservice/Italy-it_IT/navigatepub_155803_-3679/Nexans_wins_a_171_million_USD_order_to_supply_extr.html)
- 17 Tema Report: 'Rapporto sui costi medi degli impianti di rete'. Available at <https://www.web.archive.org/web/20151011164435/http://www.terna.it/LinkClick.aspx?fileticket=0UQeGAQTU81%3D&tabid=106&mid=3482>
- 18 Guidi, G., Fosso, O.B.: 'Investment cost of HVAC cable reactive power compensation off-shore'. Proc. IEEE Energycon 2012 Conf., Florence, Italy, September 2012, pp. 1–6
- 19 Caruso, L., Caserta, L.: 'Prysmian secures SylWin1 project by TenneT for the cable connection of offshore wind farms in the North Sea to the German Grid', Prysmian press release, Milano, Italy, 26 January 2011. Available at <https://www.web.archive.org/web/20151007152659/http://www.prysmiangroup.com/en/corporate/press-releases/Prysmian-secures-SylWin1-project-by-TenneT-for-the-cable-connection-of-offshore-wind-farms-in-the-North-Sea-to-the-German-power-grid/>
- 20 Caruso, L., Caserta, L.: 'Prysmian secures Dolwin3 project worth in excess of € 350 M€', Prysmian press release, Milano, Italy, 26 February 2013. Available at <https://www.web.archive.org/web/20151007152303/http://www.prysmiangroup.com/en/corporate/press-releases/Prysmian-secures-Dolwin3-project-worth-in-excess-of-350-M/>
- 21 Caruso, L., Caserta, L.: 'Prysmian secures HelWin2 project worth in excess of € 200 M for the grid connection of offshore wind farms in Germany', Prysmian press release, Milano, Italy, 1 August 2011. Available at <https://www.web.archive.org/web/20151007150955/http://www.prysmiangroup.com/en/corporate/press-releases/Prysmian-secures-HelWin2-project-worth-in-excess-of-200-M-for-the-grid-connection-of-Offshore-Wind-Farms-in-Germany/>
- 22 Caruso, L., Caserta, L.: 'Prysmian secures BorWin3 Project worth in excess of € 250 M€', Prysmian press release, Milano, Italy, 15 April 2014. Available at <https://www.web.archive.org/web/20151007151358/http://www.prysmiangroup.com/en/corporate/press-releases/Prysmian-secures-BorWin3-Project-worth-in-excess-of-250-M/>
- 23 Elliott, D., Bell, K.R.W., Finney, S.J., *et al.*: 'A comparison of AC and HVDC options for the connection of offshore wind generation in Great Britain', *IEEE Trans. Power Deliv.*, doi: 10.1109/TPWRD.2015.2453233, in press
- 24 Schoenmakers, D.: 'Optimization of the coupled grid connection of offshore wind farms' (Technical University of Eindhoven). Available at [https://www.web.archive.org/web/20151107091436/http://www.lr.tudelft.nl/fileadmin/Faculteit/LR/Organisatie/Afdelingen\\_en\\_Leerstoelen/Afdeling\\_AEWE/Wind\\_Energy/Education/Master\\_Projects/Finished\\_Master\\_projects/doc/Dirk\\_Schoenmakers\\_p.pdf](https://www.web.archive.org/web/20151107091436/http://www.lr.tudelft.nl/fileadmin/Faculteit/LR/Organisatie/Afdelingen_en_Leerstoelen/Afdeling_AEWE/Wind_Energy/Education/Master_Projects/Finished_Master_projects/doc/Dirk_Schoenmakers_p.pdf)
- 25 Torsten, T.: 'Socket out of service', Offshorewindindustry news, 9 May 2014. Available at <https://www.web.archive.org/web/20151011164732/http://www.offshorewindindustry.com/news/socket-out-service>
- 26 Block, M., Fischer, M.: 'Störung der Offshore-Netzansbindung BorWin1: Task Force arbeitet an Lösung', TenneT press release (in German), München, Germany, 07 July 2014. Available at [https://www.web.archive.org/web/20151011165648/http://www.tennet.eu/de/fileadmin/downloads/news/20140707\\_PM-Task-Force-fuer-BorWin1.pdf](https://www.web.archive.org/web/20151011165648/http://www.tennet.eu/de/fileadmin/downloads/news/20140707_PM-Task-Force-fuer-BorWin1.pdf)
- 27 CIGRE TB 379: 'Update of service experience of HV underground and cable systems', WG B1.10, 2009
- 28 CIGRE TB 513: 'Reliability of high voltage equipment – part 5 – gas insulated switchgear', WG A3.06, 2012
- 29 CIGRE TB 537: 'Guide for transformer fire safety practices', WG A2.33, 2013
- 30 CIGRE study committee B4: 'A survey of reliability of HVDC systems throughout the world during 2011–2012'. Proc. CIGRE General Session 2014, Paper B4-117, Paris, France, 24–29 August 2014
- 31 Colla, L., Marelli, M., Lauria, S., *et al.*: 'Submarine cable connections in the Mediterranean Sea: system and technological aspects'. AEIT Annual Conf., Mondello, Italy, October 2013, pp. 1–6
- 32 Donkers, J.A.J., Brand, A.J., Eecen, P.J.: 'Offshore wind atlas of the Dutch part of the North Sea'. Proc. Int. Conf. on EWEA 2011, Brussels, Belgium, March 2011, pp. 1–6
- 33 Weisse, R., Bisling, P., Gaslikova, L., *et al.*: 'Climate services for marine applications in Europe', *Earth Perspect.*, 2015, **2**, p. 3